Gating current kinetics in *Myxicola* giant axons

Order of the back transition rate constants

L. Goldman
Department of Physiology, School of Medicine, University of Maryland, Baltimore, Maryland 21201 USA

ABSTRACT Gating current, I_g, was recorded in *Myxicola* axons with series resistance compensation and higher time resolution than in previous studies. I_g at ON decays as two exponentials with time constants, $\tau_{ON\text{-}F}$ and $\tau_{ON\text{-}S}$, very similar to squid values. No indication of an additional very fast relaxation was detected, but could be still unresolved. I_g at OFF also displays two exponentials, neither reflecting recovery from charge immobilization. Deactivation of the two I_{ON} components may proceed with well-separated exponentials at −100 mV. I_{Na} tail currents at OFF also display two exponentials plus a third very slow relaxation of 5–9% of the total tail current. The very slow component is probably deactivation of a very small subpopulation of TTX sensitive channels. At −100 mV, means for I_{Na} tail component time constants (four axons) are 76 μs (range: 53–89 μs) and 344 μs (range: 312–387 μs), and for I_{OFF} (six axons) 62 μs (range: 34–87 μs) and 291 μs (range: 204–456 μs) in reasonable agreement. I_{Na} ON activation time constant, τ_A, is clearly slower than $\tau_{ON\text{-}F}$ at all potentials. Except for the interval −30 to −15 mV, τ_A is clearly faster than $\tau_{ON\text{-}S}$, and has a different dependency on potential. $\tau_{ON\text{-}S}$ is several fold smaller than τ_h. Computations with a closed$_2$ ⟷ closed$_1$ ⟷ open activation model indicated Na tail currents are consistent with a closed$_1$ ⟷ open rate constant greater than the closed$_2$ ⟷ closed$_1$.

INTRODUCTION

The nonlinear portion of the membrane displacement current, first described in nerve fibers by Armstrong and Bezanilla (1973), is at least largely the electrical sign of the operation of the channel gating machinery (Bezanilla and Armstrong, 1974; Taylor and Bezanilla, 1983; see also Armstrong, 1981 for a review of this evidence). An encouraging development for the analysis of these gating currents is the growing consensus among different laboratories as to their general experimental properties. In particular there is now fairly broad agreement that the ON of the gating current, seen during depolarizating steps in potential, decays as more than one exponential. Two or more relaxations in I_{ON} have been reported for the giant axons of squid (Armstrong and Bezanilla, 1975; Kimura and Meves, 1979; Keynes and Kimura, 1983) and crayfish (Starkus et al., 1981; Swenson, 1983), frog myelinated fibers (Nonner et al., 1978; Dubois and Schneider, 1982; but not in rabbit myelinated fibers, Chiu, 1980), skeletal muscle fibers (Campbell, 1983), and cardiac Purkinje cells (Hanck et al., 1990). In contrast I_{ON} in *Myxicola* axons has consistently been reported to decay as only a single exponential (Bullock and Schauf, 1978, 1979; Schauf and Bullock, 1979; Schauf, 1983, 1987).

I present here recordings of gating currents in *Myxicola* obtained under series resistance compensation. I_{ON} in the present study rises to its peak some four to six fold faster than previously reported. Under these recording conditions I_{ON} decays as two well-separated exponentials whose values agree very closely over a broad range of potentials with those reported for squid. These results reduce the apparent diversity in gating current properties reported among different preparations. A preliminary report of some of these findings has been made (Goldman, 1990).

METHODS

Preparation and electrical recording

Myxicola infundibulum were obtained from R. Bosien (Cummings Cove, Deer Island, New Brunswick, Canada). Methods for preparing and electrically recording from the giant axons were as described by Binstock and Goldman (1969). Axon diameters before internal perfusion ranged from ~350 to 650 μ. Normal artificial sea water (ASW) contained 440 mM Na, 10 mM Ca, 50 mM Mg, 560 mM Cl, 5 mM Tris (tris [hydroxymethyl]aminomethane; Sigma Chemical Co., St. Louis, MO), pH 8.0 ± 0.05. Temperature was 5 ± 0.5°C. Potentials are reported as absolute membrane potential (inside minus outside) and have been corrected for liquid junction potentials as described by Ebert and Goldman (1975). Sodium currents, I_{Na}, were recorded in bathing media with the Na concentration reduced by substitution with Tris to either two-thirds or one-half of that in ASW. Gating currents, I_g, were recorded in Na-free Tris ASW containing 1 or 2 μM tetrodotoxin (TTX; Calbiochem-Behring Corp., San Diego, CA). All Tris containing solutions were made freshly every two weeks.

Internal perfusion

Internal perfusion was initiated with the KCl-axoplasm dispersal method of Goldman and Kenyon (1979). All experiments for both I_g and I_{Na} were done with Cs internal perfusate containing 410 mM Cs, 50 mM F, 360 mM glutamate, 1 mM Hepes (*N*-2-hydroxyethylpiperazine

0006-3495/91/03/574/16 $2.00

N'-2-ethane sulfonic acid; Calbiochem-Behring), 4 mM EGTA (ethyleneglycol-bis-[β-amino-ethyl ether] N, N'-tetra acetic acid; Sigma Chemical Co.), 165 mM sucrose, pH 7.30 ± 0.05. The Cs perfusate was essentially (within 1%) isosmotic to the Tris ASW bathing medium (osmette A; Precision Systems Inc., Sudbury, MA). Best recordings of I_g were obtained under isosmotic conditions. Perfusates made even 5–6% hypertonic with sucrose increased the leak conductance. A few initial experiments were done with slightly hypotonic internal perfusates (Stimers et al., 1987) with no obvious effect on clamp setting time. For I_g recordings the leak conductance typically ranged from ~0.30 to 1.0 m mho/cm^2. Internal perfusates were freshly prepared at 1–2-wk intervals.

Data acquisition

Unless specifically noted otherwise (Fig. 3), all voltage clamp observations were made using compensation for the series resistance, R_s, as described by Goldman (1986). All I_{Na} recordings were made in low Na bathing media to further reduce R_s errors. With the current densities encountered in these experiments displacements in membrane potential, once the clamp has settled, produced by any residual uncompensated R_s will generally be well < 1 mV, and in no case > 2 mV.

Pulses sent to the voltage clamp were formed by a PDP 11/34 computer (Digital Equipment Corp., Maynard, MA). Membrane currents were filtered at 25 or 50 KHz for I_{Na} and 80 or 100 KHz for I_g recordings with a four pole Bessel filter (model 4302; ITHACO Inc., Ithaca, NY), digitized at a 20- or 25-μs sampling interval for I_{Na} and a 5-μs interval for I_g with a 12-bit analog to digital converter (model ADC-EH12B3; Datel Systems Inc., Canton, MA) and stored on hard disks for later analysis. A modification of the data acquisition system for I_g recordings was to include optical isolators (model HCPL 2602; Hewlett-Packard Co., Palo Alto, CA) in the data lines from the computer to the digital to analog converter.

Extraction of I_{Na}

For all experiments Na currents were extracted by repeating the entire voltage clamp protocol in either 1 or 2 μM TTX and subtracting the two sets of records with the aid of the PDP-11/34. In addition, for currents recorded during depolarizing steps (but not for I_{Na} tails at OFF) linear leak and capacitative currents for both normal and TTX controls were first subtracted by summing each depolarizing step in potential with four hyperpolarizing steps, each one-fourth of the depolarizing step (divided pulse procedure), and then proceeding with TTX subtraction. Divided pulses were used as all holding potentials were at −100 mV. To minimize any effects of slow inactivation on I_{Na} (Rudy, 1981) the preparation was held at the fixed −100 mV holding potential for 2 min before the start of each voltage clamp run, and 15 s were allowed between each voltage clamp pulse. For I_{Na} experiments the internal perfusate contained 40 mM tetraethylammonium Br (TEA; Eastman Kodak, Co., Rochester, NY) and the bathing medium 2 mM 3,4-diaminopyridine (3,4-DAP; Aldrich Chemical Co., Milwaukee, WI).

Extraction of I_g

I_g was obtained by summing, usually 20, depolarizing steps in potential from a −100 mV holding potential to the desired test potential with an equal number of 50 mV hyperpolarizing steps from a reference potential of −130 to −180 mV. Currents from the hyperpolarizing step were scaled by the factor (amplitude of the depolarizing step/50) before summing, and the resultant currents were averaged over the 20 iterations. Holding currents were zeroed for both de- and hyperpolarizing steps by presenting a blank with no potential step at the appropriate holding potential immediately before each sweep with a step and subtracting the blanks from the currents with steps. A variation on the procedure for larger test steps was to present several (usually four) hyperpolarizing steps for each depolarizing test step and to average the hyperpolarizing currents before scaling and summing. In this way the additional noise generated by large scaling factors was reduced. A critical addition for I_g recordings was the summing of each raw current trace, before filtering and digitizing, with a transient signal of up to three independent adjustable time constants and of an amplitude proportional to the de or hyperpolarizing voltage step amplitude. This reduced the amplitude of the linear capacitative current and prevented saturation of the ADC. Recordings from a passive circuit, including R_s compensation, with these same procedures produced nearly perfect subtraction, leaving only a small signal lasting no more than 10 μs. In control experiments I_g obtained by presenting iterations at 1/s and those obtained at 1/3s were identical, i.e., there was no sign of any slow inactivation of I_g at these repetition rates, possibly owing to the brief (2 ms) test steps used. Rudy (1976) found it was necessary to pulse at 10/s to reduce I_g in *Myxicola* by 15%. All the data reported were obtained at 1/3 s. In a few early I_g experiments TEA and 3,4-DAP were included, but it was found that neither of these K-channel blockers had any obvious effect on I_g in Cs perfusates.

Analysis

Time constants were fitted to both I_{Na} and I_g records as a series of exponentials description with the aid of the PDP 11/34 using patternsearch, a nonlinear least squares minimization procedure (see Colquhoun, 1971).

RESULTS

The I_{ON} response

Fig. 1 presents a typical set of I_g records, all from the same axon. Currents during a series of depolarizing steps from a −100 mV holding potential to test potentials of −30 to 70 mV are shown. In all experiments the asymmetry current continued to increase with the amplitude of the potential step, and never showed any indication of saturation or reversal.

The currents of Fig. 1 are similar to these reported for other preparations. There is a steady-state outward current component, more evident for larger depolarizing steps, which probably arises from nonlinearities in the leak current-voltage relation. Leak pedestals are also seen in squid (Armstrong and Benzanilla, 1974; Keynes and Royas, 1974; Meves, 1974), crayfish (Starkus et al., 1981; Swenson, 1983), frog myelinated fibers (Neumcke et al., 1976), rabbit myelinated fibers (Chiu, 1980), frog skeletal muscle (Campbell, 1983), and canine cardiac Purkinje cells (Hanck et al., 1990). Time to peak current was typically 20–35 μs which compares reasonably with other contemporary values (Keynes and Kimura, 1983; Stimers et al., 1987; Nonner, 1980; Chiu, 1980; Campbell, 1983; Alicata et al., 1989; Hanck et al., 1990).

Time to peak current and the effect of R_s compensa-

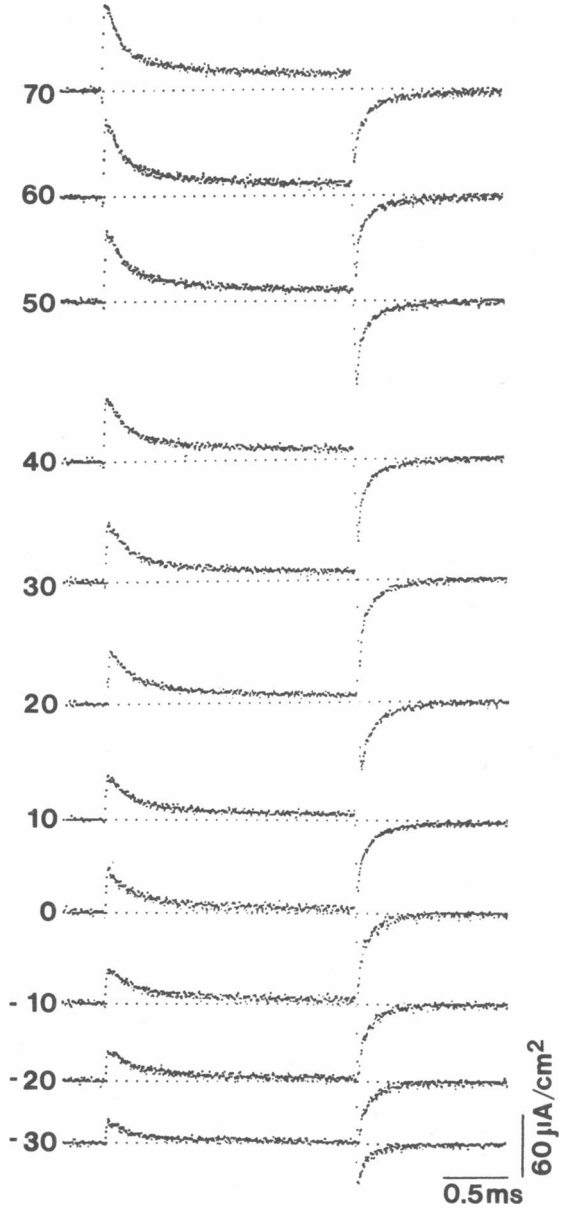

FIGURE 1 $I_g(t)$ records obtained from a single axon. Asymmetry currents during and following a 2-ms step to the indicated potentials are shown. Filtered at 80 KHz. Axon 9A26.

tion on it are shown more clearly in Fig. 2. Superimposed traces from another preparation are shown at an expanded time scale. At each potential, records are shown with and without R_s compensation. Times to peak with R_s compensation ranged from ~25 to 37 μs in this experiment. Without R_s compensation up to an additional 45 μs is needed to reach peak, producing a pronounced rising phase in agreement with the findings of Stimers et al. (1987) and Alicata et al. (1989). For test steps negative to −10 mV, currents with and without R_s compensation were indistinguishable in this experiment. The remaining rise time seen under R_s compensation most likely arises from the residual setting time of the membrane potential, although the possibility of a contribution from a genuine (albeit small) rising phase cannot be excluded. What is unlikely to be a major contributor to the residual rise time is nonlinear charge movement during the subtracting (hyperpolarizing) pulse. Control experiments in which gating currents obtained with the usual −130 to −180 mV subtracting pulse were compared with those from the same axon obtained with a −100 to −150 mV subtracting pulse revealed no appreciable differences for steps negative to 10 mV and clear effects only at and positive to 30 mV. Differences at more positive steps arise from the larger scaling factors on the subtracting pulse currents needed in this range and the consequent amplification of the small asymmetry current produced on the step from −100 to −150 mV.

Another similarity between the records of Fig. 1 and those reported for other preparations is that I_g does not decay as a single exponential. This is demonstrated in Fig. 3. The 50 mV trace from the experiment of Fig. 1 is presented three times. In the top trace a single exponential with a time constant, τ_{ON}, of 597 μs (thin curve) has been fitted to the record between 500 and 2,000 μs (indicated by vertical lines). The exponential does not fit the record at early times. Correspondingly, a single exponential fitted between 75 and 275 μs (middle trace, τ_{ON} of 185 μs) deviates from the experimental record at longer times, while a simultaneous two exponential fit between 75 and 2,000 μs well describes the entire record (bottom trace, $\tau_{ON\text{-}F}$ of 98 and $\tau_{ON\text{-}S}$ of 607 μs).

Pooled values for $\tau_{ON\text{-}F}$ and $\tau_{ON\text{-}S}$ as a function of membrane potential are shown in Figs. 5 and 6, respectively (*open circles,* data pooled from six preparations). For both the fast and slow components time constants first increase with potential from −30 to about −10 or 0 mV, are relatively potential insensitive from this value to ~40 mV, and then decline again. Values for both components are essentially indistinguishable from those reported for squid when compared at similar temperatures (Benzanilla and Armstrong, 1975; Armstrong and Bezanilla, 1975, 1977; Kimura and Meves, 1979; Bezanilla et al., 1982; Keynes and Kimura, 1983; Keynes, 1986).

For the record of Fig. 3 the amplitude of the slow component was 0.33 of the fast. This was a typical value. More than half the records had ratios between 0.25 and 0.40, but they could vary from a low of 0.16 to values greater than unity. The point is that neither component is a negligible fraction of the other. Schauf and his collaborators were never able to resolve more than one relaxation in I_{ON} in *Myxicola,* although some effort was

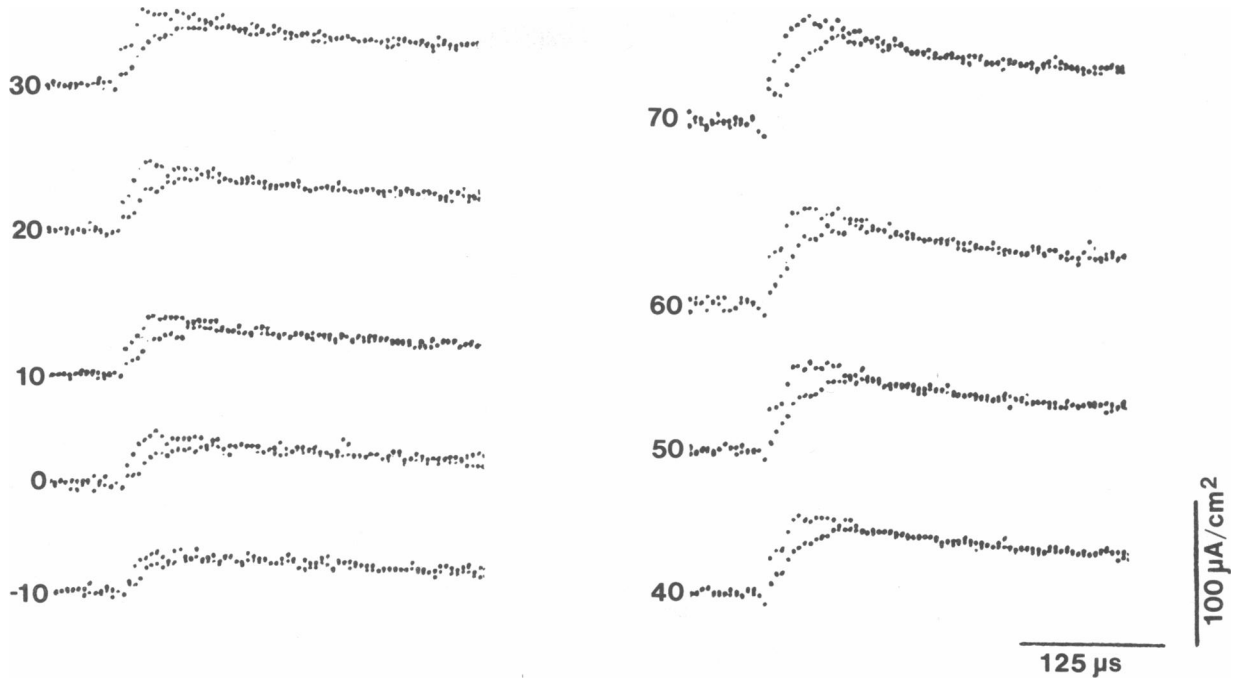

FIGURE 2 Superimposed $I_g(t)$ records obtained with and without R_s compensation. Compensation reduces the time-to-peak current by up to 45 µs, although effects are less for smaller test steps in potential and were negligible for steps negative to −10 mV in this experiment. Filtered at 80 KHz. Axon 9A27.

made to do so (see, e.g., Bullock and Schauf, 1979). A possible basis for this discrepancy is suggested by the fact that I_{ON} here rises to peak some four to six times faster than previously reported in *Myxicola*. The earlier studies seem, then, to have been done with an appreciably slower clamp setting time and a consequent distortion of I_{ON} kinetics.

Comparison with I_{Na} kinetics

It is of interest to compare these gating current kinetics to I_{Na} activation kinetics. I_{Na} was described as a series of exponentials as for I_g. Fig. 4 presents an Na current record at −10 mV. Superimposed on the experimental trace is a simultaneous three-exponential fit from 75 µs (*vertical line*) to the end of the 25-ms step (not illustrated). Values for this fit were a delay time constant, τ_D, of 0.118 ms, an activation time constant, τ_A, of 0.382 ms, and an inactivation time constant, τ_h, of 4.99 ms. A two exponential fit to this same record starting at 275 µs gave nearly identical τ_A and τ_h values of 0.408 and 4.97 ms. Hence, τ_A can be reliably determined without resolving τ_D, i.e., the exponentials are well separated. A similar conclusion was reached by Goldman (1989). τ_D is not reliable in these experiments. It is not known with any certainty how many delaying processes there are, very fast relaxations cannot be accurately resolved in these data, and three exponential fits require three to four-fold more iterations than do two exponential fits.

τ_A values (two exponential fits) pooled from four axons are shown in Figs. 5 and 6 (*crosses*). The solid curves are both τ_m (V) taken from Goldman and Schauf (1973), and have not been fitted to these data. τ_A (V) and τ_m (V) agree quite closely even though the different methods of their extration imply quite different relationships between activation and inactivation. Keynes (1986) made a similar observation. Neither $\tau_{ON\text{-}F}$ or $\tau_{ON\text{-}S}$ are identical with τ_A, and there is no recognized process in I_g with the kinetics of Na activation over the whole potential range examined. This same sort of discrepancy has been reported for other preparations (see Discussion). From −30 to about −15 mV $\tau_{ON\text{-}S}$ and τ_A values do overlap (Fig. 6), although $\tau_{ON\text{-}S}$ is increasing and τ_A decreasing with potential in this overlap range. $\tau_{ON\text{-}S}$ in this range, then, seems to correspond to the intermediate component of Armstrong and Gilly (1979). $\tau_{ON\text{-}S}$ is considerably faster than τ_h which ranged from 5.72–7.21 ms at −20 mV and 3.46–5.20 ms at 40 mV.

No very fast I_{ON} relaxation is detected

Fig. 7 presents an I_g record at 20 mV shown at a very expanded time scale. Superimposed on the experimental trace is the usual simultaneous two exponential fit,

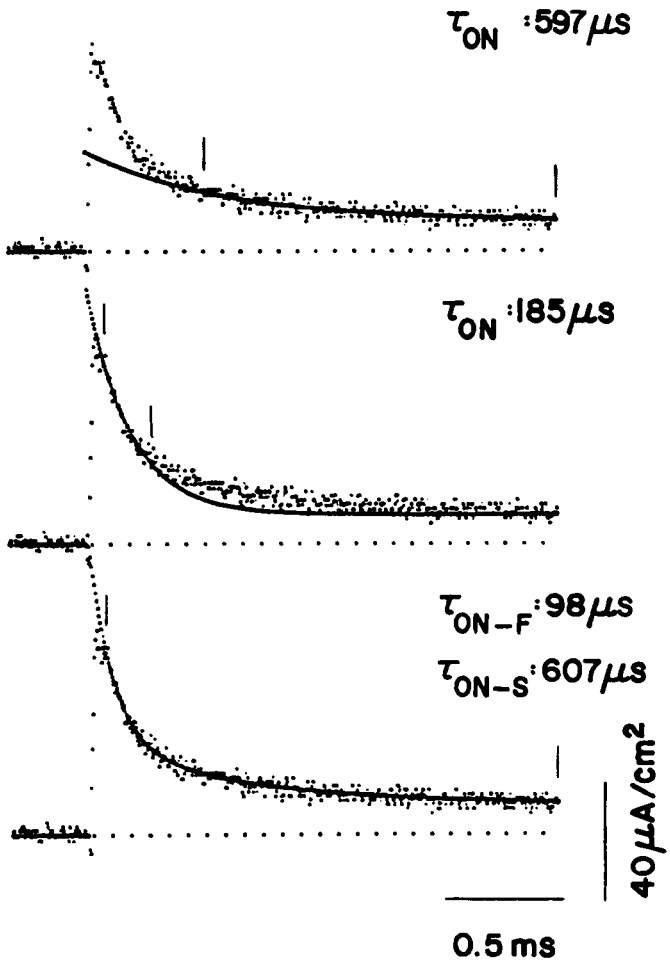

FIGURE 3 I_{ON} record for the step to 50 mV of Fig. 1. The trace is presented three times. In the top trace a single exponential (*thin curve*, τ_{ON} of 597 μs) has been fitted between 500 μs into the step and the end of the 2-ms step (*vertical lines*). In the middle trace a single exponential (τ_{ON} of 185 μs) has ben fitted between 75 and 275 μs. In neither case does the single exponential fit provide a good description of the whole experimental record. A good fit is provided (*lower trace*) with a two exponential fit given by $I_g(t) = 68.5 \exp(-t/0.098) + 22.8 \exp(-t/0.607) + 9.7$, with I_g in microamperes per centimeter squared and t in milliseconds.

extrapolated to the beginning of the step. The fit was started at 75 μs (*arrow*), and well describes the experimental record up through the time of peak current at 30 μs. Fitting again with the two exponentials, but now starting at 125 μs produced the same result, a good fit up through the 30-μs point. This result has two implications. First, membrane potential seems to have essentially fully settled by the time of peak current. This was found to be the case over most of the potential range examined. For very positive steps there was often a small creep up to the fitted exponential. Second, there is no sign of an additional very fast I_{ON} relaxation, as described by Forster and Greeff (1990) in squid. These result do not establish that there is no fast I_{ON} relaxation in *Myxicola*. It could be too fast to resolve in these experiments, or alternatively not sufficiently separated from $\tau_{ON\text{-}F}$. However, the experimental finding is clear. I was never able to demonstrate a very fast relaxation under these recording conditions.

The I_{OFF} response

There are also slow and fast components in the I_{OFF} response. Fig. 8 shows the OFF response for the record of Fig. 3. The same trace is presented three times. In the upper trace a single exponential (thin curve, τ_{OFF} of 251 μs) has been fitted to the experimental record for 300 μs (*vertical line*) to 2.8 ms (not illustrated). The fitted exponential does not describe the experimental record at early times. In the middle trace a single exponential fitted between 50 and 150 μs (*vertical lines*, τ_{OFF} of 118 μs) does not describe the experimental record at intermediate times. A good fit to the entire record is provided by a simultaneous two exponential fit (lower trace, $\tau_{OFF\text{-}F}$ of 68 and $\tau_{OFF\text{-}S}$ of 267 μs).

Values for $\tau_{OFF\text{-}F}$ and $\tau_{OFF\text{-}S}$ all at −100 mV are presented in Table 1 for the six axons analyzed. Armstrong and Bezanilla (1977) found that I_{OFF} in squid decayed as a single exponential at −70 mV, while at −140 or −150 mV, where the recovery from Na inactivation is rapid, a second slower component was recognized. They presented compelling evidence that their slow I_{OFF} component is related to recovery from charge immobilization. At the more negative potentials the ratio of the integral of $I_{OFF}$to I_{ON}, Q_{OFF}/Q_{ON}, was always equal to or greater than unity when the slow OFF component was included. Very similar results were reported from skeletal muscle fibers (Campbell, 1983) and rabbit myelinated fibers (Chiu, 1980), and also indicated in crayfish axons (Starkus et al., 1982) and frog myelinated fibers (Pohl, 1989).

The slow I_{OFF} component at −100 mV described here does not seem to be associated with recovery from immobilization. For the record of Figs. 3 and 8 Q_{ON} at the end of the 2 ms step, determined from the time constants and zero time intercepts for both fitted exponentials, corrected for this step duration, was 20.0 nC/cm², while Q_{OFF} including both components was 9.2 nC/cm² for a Q_{OFF}/Q_{ON} of 0.46. There is, then, substantial charge immobilization even when the slow OFF component is taken into account. This was generally the case except for very small depolarizing steps where Q_{OFF} could be about equal to Q_{ON}. Q_{OFF}/Q_{ON} values following different test potentials are shown for three axons in Table 2. For *Myxicola* both OFF components at −100 mV may be associated with activation. This possibility is supported by observations on the Na tail current.

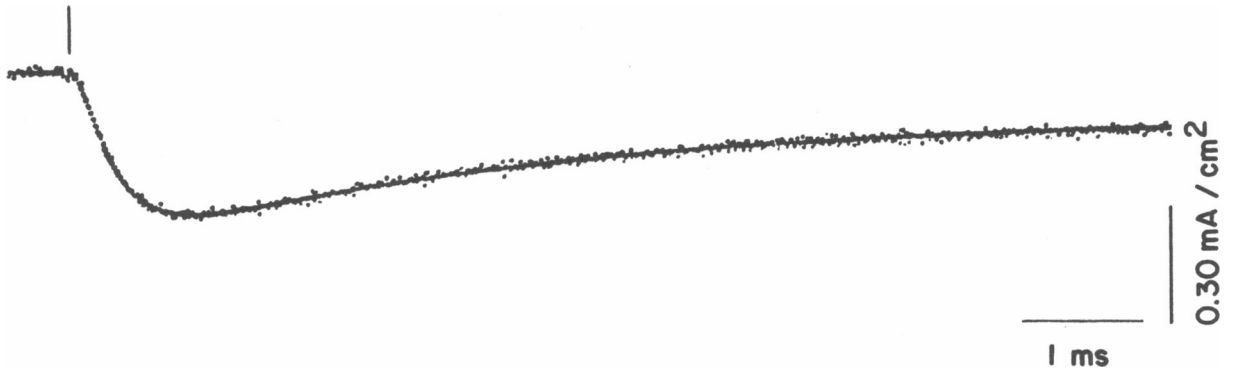

FIGURE 4 I_{Na} record for a step to −10 mV. Superimposed on the experimental record is a three exponential fit started at 75 μs (*vertical line*) given by $I_{Na}(t) = 442.0 \exp(-t/0.118) - 864.8 \exp(-t/0.382) + 384.0 \exp(-t/4.99) + 103.3$, with I_{Na} in μA/cm² and t in milliseconds. 2/3 Na ASW. Axon 7A27.

Na tail currents

There are three relaxations in Na tail currents at OFF recorded at −100 mV. Fig. 9 presents the same tail current record twice. In the upper trace a two exponential fit (*thin curve*) from 500 μs (*vertical line*) to 11.5 ms (not illustrated) has been superimposed. Values were 364 μs for the slow relaxation, τ_S, and 3.36 ms for the very slow relaxation, τ_{VS}. The two exponential fit does not describe the early time course of the tail current. The lower trace shows that a good description of the whole experimental record is provided by a three exponential fit (τ_F of 73 μs, τ_S of 330 μs, and τ_{VS} of 3.30 ms). Values for τ_F and τ_S for each of the four axons analyzed are given in Table 3.

A very slow time constant in Na tail currents in squid, with values very similar to τ_{VS}, was reported by Gillespie and Meves (1980), and analyzed by Gilly and Armstrong (1984). Gilly and Armstrong identified this component as the OFF response for a small subpopulation of Na

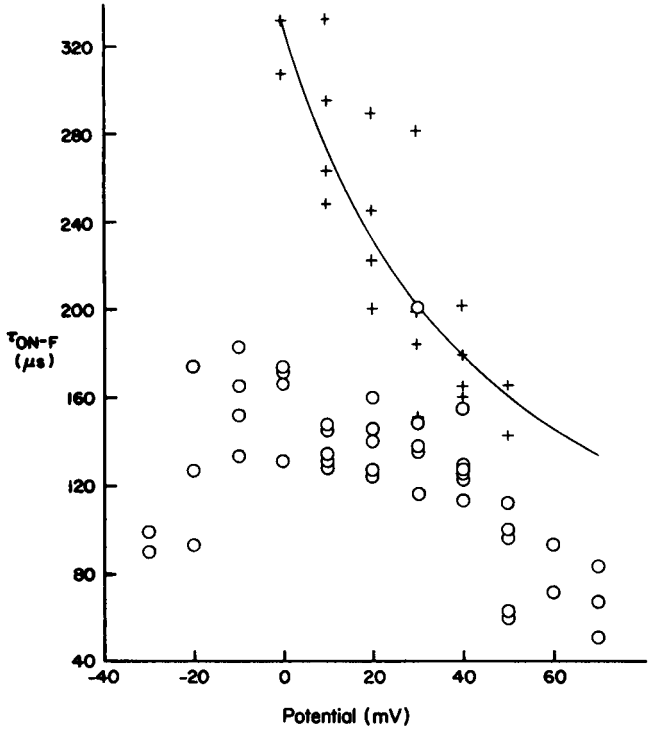

FIGURE 5 $\tau_{ON\text{-}F}$ as a function of membrane potential (*open circles*). Collected values from six experiments. Crosses indicate τ_A values from Na current records, and the solid curve is $\tau_m(V)$ from Goldman and Schauf (1973).

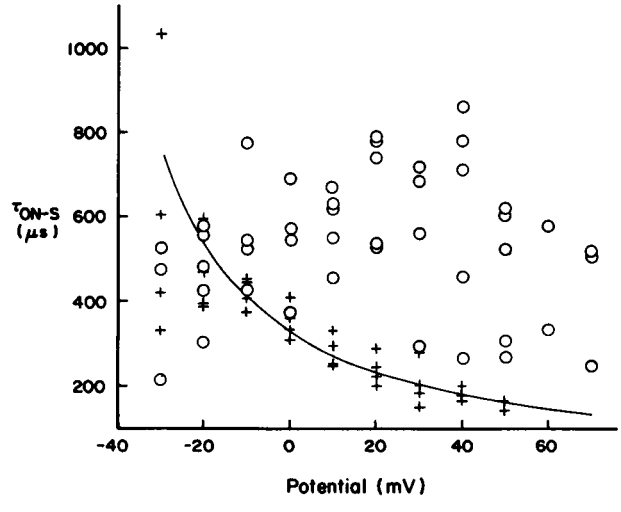

FIGURE 6 $\tau_{ON\text{-}S}$ as a function of membrane potential (*open circles*, six experiments). Crosses (data pooled from four experiments) and solid curve as for Fig. 5.

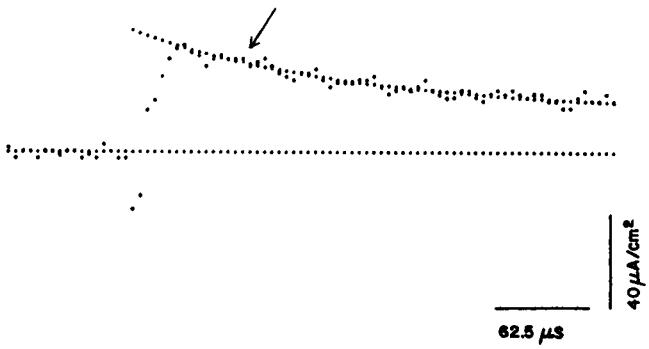

FIGURE 7 I_{ON} record at 20 mV shown at an expanded time scale. Superimposed (*thin curve*) is a two exponential fit started at 75 μs (*arrow*). The fitted curve extrapolated through the peak current point at 30 μs, suggesting essentially full setting of the clamp potential by this time. Same axon as for Fig. 2.

channels with different kinetics from and activated at more negative potentials than the main population. Currents from these "threshold" channels are generally not detectable for test steps positive to about −30 to −40 mV as the increasing activation from the main population reduces then contribution to a small fraction of the total I_{Na}. A small subpopulation of TTX-sensitive channels with very similar properties to these threshold channels had also been described in *Myxicola* (Goldman and Hahin, 1978). It seems likely that the very slow tail current component described here also generates from this small subpopulation. Gilly and Armstrong found that the subpopulation tail current amplitude was ~3% of the total Na tail current, and I find ~5–9%. If indeed the very slow OFF response generates from this subpopulation, then both the fast and slow I_{Na} tail components must be deactivation of the main population of channels. There are, then, two components in the OFF response for both I_g and I_{Na}.

Mean values for τ_F and τ_S are 76 and 344 μs, respectively (Table 3). Goldman and Hahin (1978) reported two components in I_{Na} tail currents in *Myxicola*. At −100 mV their values were 92–107 μs for the fast and 1.0–1.28 ms for the slow component. For the fast component the two sets of values are not very different. However, the slow components differ by a factor of 3. This must be because Goldman and Hahin did not recognize the very slow component in their tail current records, and their fast component was somewhat and their slow heavily contaminated by this very slow relaxation. Mozhaeva et al. (1980), Nonner (1980), and Sigworth (1981) in frog myelinated fibers, Hahin (1988) in frog skeletal muscle fibers, and Alicata et al. (1990) in crayfish also described two components in Na tail currents.

Mean value for the fast Na tail relaxation is 76 μs with

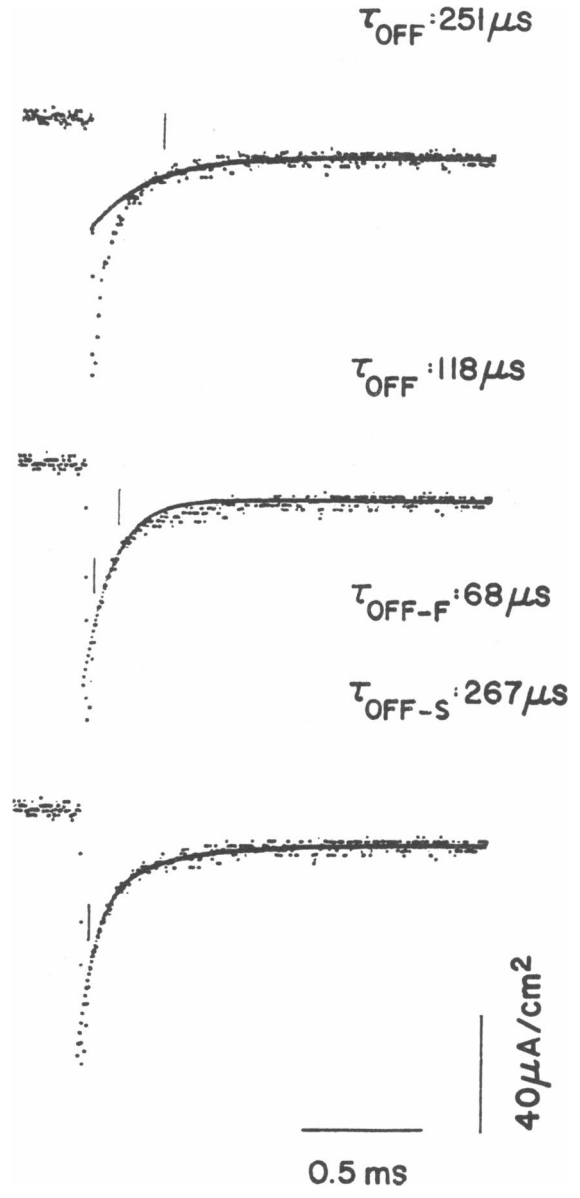

FIGURE 8 I_{OFF} for the same record as Fig. 3. The trace is presented three times. In the top trace a single exponential (*thin trace*, τ_{OFF} of 251 μs) has been fitted to the record starting at 300 μs (*vertical line*). A single exponential has been fitted between 50 and 150 μs in the middle trace (τ_{OFF} of 118 μs). In neither case does the single exponential provide a good description of the whole experimental record. A good description is provided with a two exponential fit (*lower trace*) given by $I_g(t) = 50.2 \exp(-t/0.068) + 21.9 \exp(-t/0.267)$, with I_g in μA/cm² and t in milliseconds.

a range of 53–89 μs, and that for the slow component is 344 μs (range: 312–387 μs). Corresponding values for the two I_{OFF} components are 62 μs (range: 34–87 μs) and 291 μs (range: 204–456 μs). These values are in reasonable agreement for both components and provide the

TABLE 1 I_g at OFF fitted parameters

Axon	$\tau_{OFF\text{-}F}$	$^*I_{O\text{-}F}$	$\tau_{OFF\text{-}S}$	$^*I_{O\text{-}S}$	$I_{O\text{-}S}/I_{O\text{-}F}$
	μs	$\mu A/cm^2$	μs	$\mu A/cm^2$	
9A23	34	33.6	247	22.7	0.68
9A11	46	46.4	456	8.0	0.17
9A27	47	51.1	204	15.4	0.30
9A25	75	21.9	239	10.1	0.46
9A22	83	29.7	305	16.5	0.56
9A26	87	49.6	296	15.9	0.32
MEAN	62.0		291.2		0.415

All values were determined at −100 mV following 2-ms test steps in potential.
Values are means following test steps from 10 to 70 mV.
*Zero time intercept of fast and slow fitted exponentials.

clearest evidence that these asymmetry currents are indeed largely associated with Na channel gating.

DISCUSSION

I_{ON} rises to peak considerably faster than had been reported for *Myxicola,* and its properties are consequently different from those previously described. This seems, then, to be the first report of gating currents in *Myxicola* recorded with sufficient time resolution to identify the major components. Significant information about gating is contained in the first 100–200 μs following a step in potential, and currents in this time interval were largely unresolved previously. Kinetics of I_g for both ON and OFF responses have therefore been described in some detail.

TABLE 2 $^*Q_{OFF}/Q_{ON}$ following various test potentials

‡Test potential	Axon		
	9A23	9A26	9A27
mV			
−10	0.92	0.62	0.81
0	0.61	0.65	0.72
10	0.61	0.67	0.61
20	0.66	0.52	0.59
30	0.57	0.54	0.61
40	0.54	0.53	0.65
50	—	0.46	0.55
60	—	0.46	0.62
70	0.55	0.46	0.68

Q_{OFF} was always determinted at −100 mV.
*Q_{OFF} and Q_{ON} are the integrals of I_{OFF} and I_{ON}, respectively, determined from the time constants and zero time intercepts of the fitted exponentials, corrected for the 2-ms test step duration. Slow and fast components are included for both ON and OFF responses.
‡Potential at which Q_{ON} was determined.

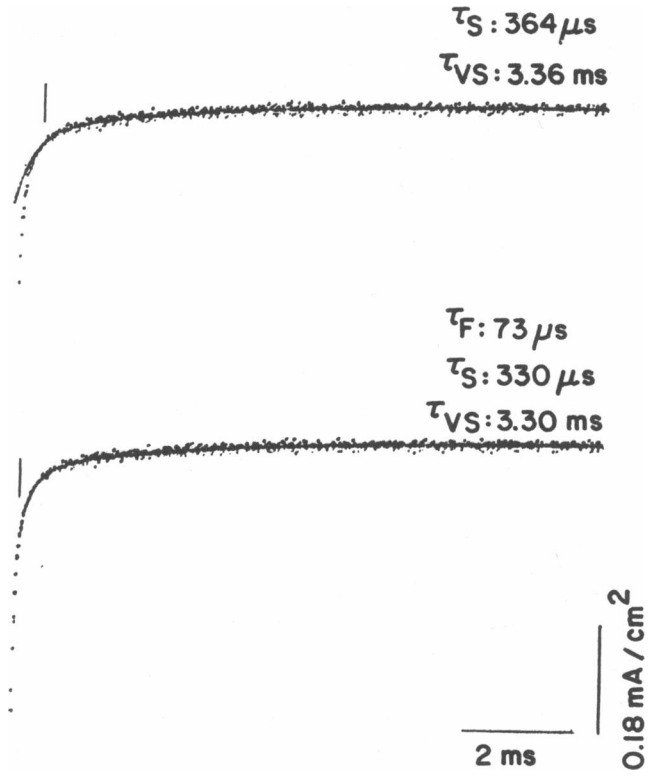

FIGURE 9 I_{Na} tail current following a 3-ms step to −10 mV. The same record is presented twice. A good description of the whole record is not provided with a two exponential fit (upper trace, τ_S of 364 μs and τ_{VS} of 3.36 ms), but is with a three exponential fit (*lower trace*) given by $I_{Na}(t) = 610.9 \exp(-t/0.073) + 139.7 \exp(-t/0.330) + 66.5 \exp(-t/3.30)$, with I_{Na} in μA/cm² and t in milliseconds. 1/2 Na ASW. Axon 7A1.

There are two resolved relaxations in the I_{ON} response

A central finding is that I_{ON} decays as two well-separated exponentials whose time constants are essentially indistinguishable from these in squid. Two or more relax-

TABLE 3 I_{Na} at OFF fitted parameters for fast and slow components

Axon	τ_F	$^*I_{O\text{-}F}$	τ_S	$^*I_{O\text{-}S}$	$I_{O\text{-}S}/I_{O\text{-}F}$
	μs	$\mu A/cm^2$	μs	$\mu A/cm^2$	
7A2	53	165	323	60	0.36
7A1	80	594	352	117	0.20
7A3	81	290	312	79	0.27
7A5	89	522	387	110	0.21
MEAN	75.8		343.5		0.26

All values were determined at −100 mV following 3-ms test steps to −10 mV.
*Zero time intercept of fast and slow fitted exponentials.

ations in I_{ON} are now reported for most preparations (Armstrong and Bezanilla, 1975; Kimura and Meves, 1979; Keynes and Kimura, 1983; Starkus et al., 1981; Swenson, 1983; Nonner et al., 1978; Dubois and Schneider, 1982; Campbell, 1983; Hanck et al., 1990). This is a helpful result in that it reduces the apparent diversity in gating current properties that had been reported, and may aid in the eventual identification of the nature of these relaxations.

A clear difference in I_g between *Myxicola* and squid axons is that *Myxicola* shows no sign of a very fast relaxation as has been reported in squid (Bekkers et al., 1989; Forster and Greef, 1990). This very fast component does not immobilize, and has been interpreted as arising from a charge displacement that is independent of and parallel to the main Na channel gating charge (Forster and Greef, 1990).

There are two relaxations in the I_{OFF} response

There are also two well-separated components at OFF. Two I_{OFF} components have been described under certain conditions, but in each case the slow relaxation seemed to arise from recovery from charge immobilization. The slow OFF component described here does not reflect recovery from immobilization. $\tau_{OFF\text{-}F}$ and $\tau_{OFF\text{-}S}$ may, then, be deactivation of the two ON components, i.e., the OFF exponentials may be particularly well separated in *Myxicola* at -100 mV.

Correspondingly, there are several components in Na tail currents. Neither the fast or slow component seems to arise from deactivation of the small subpopulation of TTX sensitive channels (Goldman and Hahin, 1978), and are probably both deactivation of the main population of Na channels. Two deactivation relaxations could arise from two open states (Sigworth, 1981; Hahin, 1988) or two closed states (see Appendix). There are at least two closed states as there is a delay in the rise of I_{Na}, and for this reason alone two or more tail current relaxations are expected under certain conditions. Arguments are presented below suggesting that the two OFF relaxations may arise from two closed states.

Gating current and Na current at ON

An unresolved problem in the analysis of gating currents is that for no preparation has there been an unambiguous identification of I_{ON} with I_{Na} relaxations over the whole potential range examined. The fast I_{ON} process has properties much like that delaying the rise in I_{Na} (Armstrong and Gilly, 1979; Starkus et al., 1981), although a correspondence has not been established quantitatively. What does seem to be ruled out is a correspondence between the fast ON and the Na activation, τ_A, process. $\tau_{ON\text{-}F}$ is clearly faster than τ_A (Armstrong and Gilly, 1979; Starkus, et al., 1981; Keynes and Kimura, 1983; Campbell, 1983; Hanck et al., 1990; this work).

$\tau_{ON\text{-}F}$ increases with potential over a range where the time to peak I_{Na} is decreasing. However, time to peak I_{Na} is rate limited by the τ_A process. An I_{Na} kinetic parameter with a time constant that also increases with potential over the same negative range seen for $\tau_{ON\text{-}F}$ and $\tau_{ON\text{-}S}$ was reported by Hahin and Goldman (1978) who studied the translations along the time axis produced in I_{Na} by conditioning pulses of various potentials and durations. The time course of development of the translation was described as a single exponential. Time constants for this process increased with conditioning pulse potential from -50 to ~ 0 mV. Values for this $\tau_{SHIFT}(V)$ are in rough agreement with $\tau_{ON\text{-}S}$ (V). However, it is not clear what process the τ_{SHIFT} values should be compared with. Simulations of $\tau_{SHIFT}(V)$ using m^3h kinetics (Hahin and Goldman, 1978) predicted values several fold slower than $\tau_m(V)$, and τ_{SHIFT} may well reflect the $\tau_{ON\text{-}F}$ process. Goldman and Hahin (1978) found that the time constant for the fast component in the Na tail currents also increased with potential from -50 to about -10 to -15 mV. Overall, then, there would seem to be no major difficulties in correlating the fast I_{ON} process with I_{Na} behavior, but an exact correspondence has not been established.

More serious problems are posed by $\tau_{ON\text{-}S}$. Except for a relatively brief overlap range between about -30 and -15 mV, corresponding to the intermediate component of Armstrong and Gilly (1979), $\tau_{ON\text{-}S}$ (V) and $\tau_A(V)$ do not agree. $\tau_{ON\text{-}S}$ over most of the range examined is too slow to be the Na activation time constant, and is always considerably faster than τ_h. Moreover, from about -30 to 40 mV τ_A is decreasing while $\tau_{ON\text{-}S}(V)$ is either increasing with or relatively independent of potential. We have, then, except for the overlap range, a process in the gating current that does not correspond to any known process in I_{Na}, and no I_g process that corresponds to Na activation. This has been a general finding in the study of gating currents. Armstrong and Bezanilla (1977) and Armstrong and Gilly (1979) also found that their slow ON component was too slow to correspond to Na activation, at least positive to 0–20 mV. Hanck et al., (1990) found that τ_m was faster than their slow and slower than their fast I_{ON} component at and positive to about -40 mV, while τ_m and the slow ON time constant were in reasonable agreement negative to this potential. Campbell (1983) found that τ_m was in reasonable agreement with the time constant of his slow ON response positive to 0 mV, but differed substantially at negative

potentials. Hence, squid and *Myxicola* axons, frog muscle fibers, and canine Purkinje cells all show some potential range where the slow ON time constant of the gating current and the Na activation time constant are in reasonable agreement, and other ranges where they differ substantially.

There is compelling evidence that the asymmetrical displacement current is very largely associated with Na channel gating (see, e.g., Armstrong, 1981; Nonner, 1980; Dubois and Schneider, 1982; Campbell, 1983; Swenson, 1983; Taylor and Bezanilla, 1983), yet discrepancies between gating current and Na activation kinetics are generally seen. These discrepancies are not generated by a minor component of the gating current. For the record of Fig. 3 about two-thirds of the total charge displacement is contained in the slow component, while $\tau_{ON\text{-}S}$ is 3–4 times slower than τ_A at this potential. Not surprisingly, then, even quite complex kinetic models were unable to simultaneously describe both I_g and I_{Na} time courses at all potentials (Armstrong and Gilly, 1979; Gilly and Armstrong, 1982). At positive potentials there was a slow relaxation in I_g not accounted for. These models would be even less successful in *Myxicola* as the region of overlap of $\tau_{ON\text{-}S}$ and τ_A is apparently narrower and the ratio of slow to fast I_{ON} amplitudes is typically twice that of squid.

If the Na channel gating machinery is to be described by any time homogeneous Markov process, then the relaxations in one measurement should also be in the other, if indeed I_g is nearly entirely associated with Na gating. In principle, in that case, there is no kinetic information in I_g not contained in I_{Na}. In the next section computations of both I_g and I_{Na} are made with a model with just two closed and one open state. Only activation is considered as high time resolution data on the kinetics of charge immobilization are not yet available for *Myxicola*. Three states for activation are the largest number that the available data for *Myxicola* can justify. Some effort was made to identify additional relaxations in I_{ON} (Fig. 7) without, as yet, success.

Computations of I_{Na} and I_g

The kinetic scheme is

$$\text{closed}_2 \underset{k_{12}}{\overset{k_{21}}{\rightleftharpoons}} \text{closed}_1 \underset{k_{01}}{\overset{k_{10}}{\rightleftharpoons}} \text{open},$$

where the transition rate constants, k's, are in general all different. Details of the computations including a complete description of the time course of occupancy of each of these states in terms of the transition rate constants are given in the Appendix. Using these relations all of the predicted behaviors of I_g and I_{Na} for both ON and OFF can be directly calculated, without requiring iterative methods, by just selecting values for the transition rate constants and specifying two initial conditions. For the computations presented here initial conditions are taken as full occupancy of closed$_2$ and no occupancy of the other states for all ON computations, and full occupancy of the open with no occupancy of closed states for all OFF computations. The point of these computations is first to define some of the kinetic information that can be obtained from I_{Na} and I_g time courses. Analytical solutions rather than numerical simulations are used so that properties that are inherent in the scheme and not just consequences of the particular parameters selected for computation can be identified. Second, a new finding on the relative values of the back transition rate constants at OFF is presented.

The same relaxations appear in I_{Na} and I_g

It is shown in the Appendix that $I_{Na}(t)$ and $I_g(t)$ are both described by the same two exponentials with relaxation rate constants a and b. However, the relative value of the coefficients on these exponential terms can differ in the two measurements. Fig. 10*A* (*bottom trace*) presents a simulated I_{Na} record computed with $k_{21} = 10.0\ \text{ms}^{-1}$, $k_{12} = 0.05\ \text{ms}^{-1}$, $k_{10} = 3.33\ \text{ms}^{-1}$, and $k_{01} = 0$. Setting k_{01} to zero requires that the steady-state probability of occupancy of the conducting state is unity. $I_{Na}(t)$ is described by (with I_{Na} in $\mu\text{A/cm}^2$ and t in milliseconds)

$$I_{Na}(t) = Ni_{Na}[1.0 + 0.488 \exp(-t/0.099) - 1.488 \exp(-t.0.303)], \quad (1)$$

where i_{Na} is the current through a single channel and N is the channel density. $I_g(t)$ computed with these same rate constants is shown by the upper three traces in Fig. 10*A*. With the charge displaced for every closed$_2$-closed$_1$ transition, Q_{21}, equal to that for each closed$_1$- open transition, Q_{10}, (indicated by 1:1) $I_g(t)$ is described by

$$I_g(t) = 10.0NQ_{21}[0.504 \exp(-t.0/099) + 0.496 \exp(-t/0.303)]. \quad (2)$$

Both time constants are identical, but the amplitude of the slow relaxation is about three times that of the fast in Eq. 1 while they are nearly equal in Eq. 2. The same kinetic information is contained in both measurements.

Decreasing the Q_{21}/Q_{10} ratio from 1:1 to 1:3 (Fig. 10*A*) produced a pronounced slowing, approaching a plateau, in the initial decline of $I_g(t)$, and decreasing it to 1:4 produced a clear rising phase although the rate constants were identical for all three computations. Hence, even if not artefactual (Stimers et al., 1987), the pres-

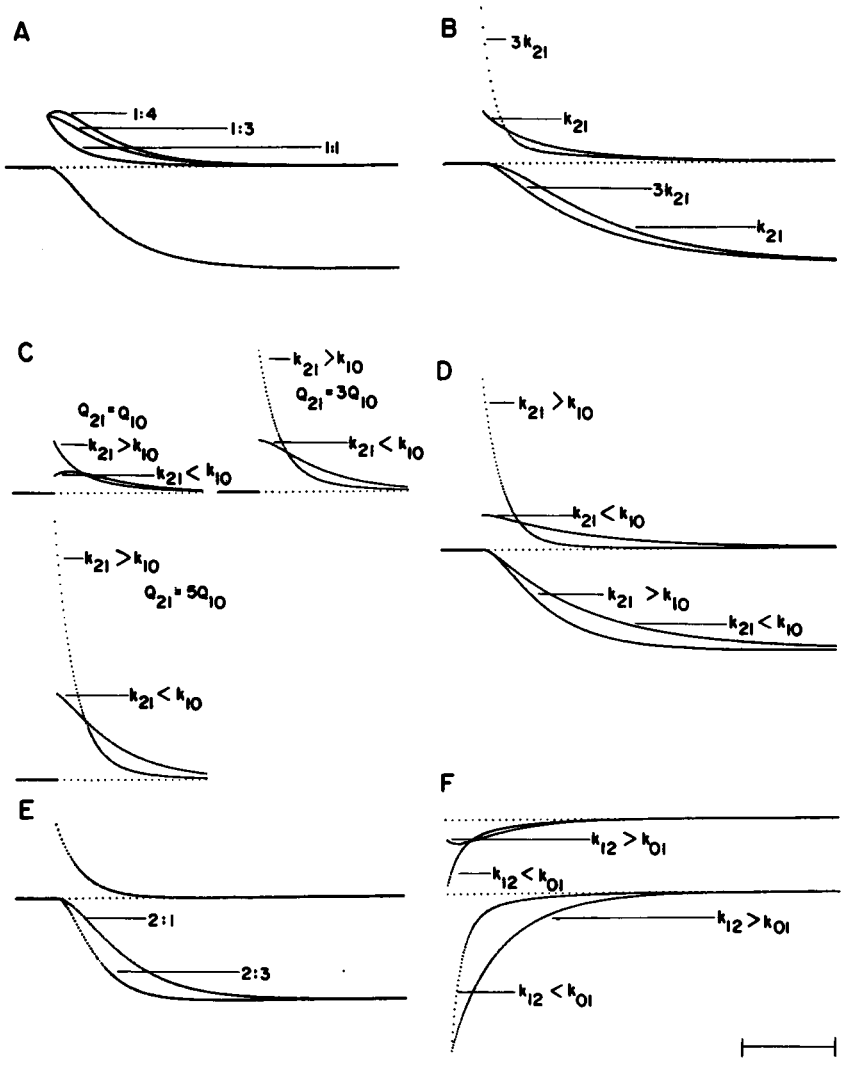

FIGURE 10 Simulations of $I_g(t)$ and $I_{Na}(t)$ computed from a sequential model with two closed and a single open state. Lower traces in parts *A*, *B*, *D*, and *E* are $I_{Na}(t)$ at ON. Upper traces in these and all traces in part *C* are $I_g(t)$ at ON. $I_{Na}(t)$ (*lower traces*) and $I_g(t)$ (*upper traces*) at OFF are shown in part *F*. Vertical scaling is arbitrary, corresponding to making no assumption as to the relative values of i_{Na} and Q_{21} (see text). However, within any part of the figure scaling is constant for any given type of measurement. Ratios in part *A* indicate values for Q_{21}/Q_{10}. Those in part *E* indicate values for k_{21}/k_{10}. Values for the transition rate constants and initial conditions in each case are given in the text. Scale: 500 μs for *A*, *C*, *D*, and *F*, 250 μs for *B* and *E*.

ence of a rising phase in I_g provides no unambiguous information as to the relative values of the transition rate constants. This is discussed further below.

The number of relaxations in I_g does not depend on the number of transitions involving charge displacement

If k_{10} and k_{01} are now assumed to be voltage independent, i.e., only the closed$_2$-closed$_1$ transition involves charge displacement, Eq. 2 becomes

$$I_g(t) = 10.0NQ_{21}\,[0.996 \exp(-t/0.099) + 0.004 \exp(-t/0.303)]. \quad (3)$$

The coefficient for the slower exponential has become negligible. This result does not mean that only transitions involving charge displacement are detectable in $I_g(t)$, but is a consequence of the particular rate constants selected. Recomputing $I_g(t)$ with $k_{21} = 6.0\ ms^{-1}$, $k_{12} = 1.8\ ms^{-1}$, $k_{10} = 5.5\ ms^{-1}$, and $k_{01} = 0$ yields with only

the closed$_2$-closed$_1$ transition involving charge displacement

$$I_g(t) = 6.0NQ_{21}\,[0.672 \exp(-t/0.100) + 0.328 \exp(-t/0.303)]. \quad (4)$$

The time constants in Eq. 4 are essentially identical to those in Eq. 3, but now the amplitude of the slow exponential is nearly half that of the fast. The relative prominence of a second relaxation is determined in part by the relative values of k_{10} and k_{21}, and the number of prominent relaxations in I_g provide no unambiguous information as to the number of transitions with voltage-dependent rate constants. Similarly, a transition governed by a small forward rate constant may make only a negligible contribution to I_g even if the rate constants have substantial voltage dependency. Hence, that a relaxation with the kinetics of inactivation is not detected in I_g does not of itself mean that the open-inactivated transition does not involve charge displacement. The slow inactivation rate constant produces a small I_g relaxation.

$I_{Na}(t)$ is sensitive to closed state transitions

Fig. 10 *B* presents two $I_{Na}(t)$ computations. The rightmost trace (indicated k_{21}) is identical to the computation of Fig. 10 *A* (but now shown at a two-fold expanded time scale) while the other ($3k_{21}$) has been computed with k_{21} increased from 10.0 to 30.0 ms^{-1}. $I_g(t)$ computations with $Q_{21} = Q_{10}$ are also shown for these two cases. $I_{Na}(t)$ clearly changes with a change only in a closed state transition rate constant. $I_g(t)$ with $k_{21} = 30.0$ ms^{-1} has better separated relaxations as the time constants are now 33 and 301 μs. It is not only I_g that contains information on closed state transitions. It is shown below that I_{Na} tail currents also contain information on closed state transitions.

An I_g rising phase does not provide unambiguous kinetic information

Armstrong (1981) and Armstrong and Matteson (1984), using a sequential model with an additional closed state, found that inverting the order of the rate constants, i.e., the relative values of the transition rate constants proceeding from left to right, produced a rising phase in $I_g(t)$. I get a similar result. Fig. 10 *C* (*top left hand panel*, indicated by $Q_{21} = Q_{10}$) presents two I_g simulations both computed with a Q_{21}/Q_{10} ratio of 1.0. The monotonically decaying trace (indicated by $k_{21} > k_{10}$) is identical to the (1:1) computation of part A above. The trace indicated $k_{21} < k_{10}$ has been computed with the values for these rate constants exchanged each for each (i.e., k_{21} is now 3.33 and k_{10} is now 10.0 ms^{-1}). There is now a rising phase of I_g.

As might be expected from the result of part A, the rising phase can be eliminated by changing the Q_{21}/Q_{10} ratio. The other two panels in Fig. 10 *C* present pairs of I_g simulations computed with the same rate constants as for the upper left panel for both the normal ($k_{21} > k_{10}$) and inverted ($k_{21} < k_{10}$) cases, but now with increased Q_{21}/Q_{10} ratios. A ratio of 3:1 reduces the rising phase to an initial plateau (*top right hand traces*), and a ratio of 5:1 leaves only a small slowing of the initial I_g decay (*lower traces*). Again, the presence or absence of a rising phase provides no unambiguous information as to the order of the rate constants. The reason for this is seen in the Appendix. I_g for any x_i-x_j transition is scaled by both Q_{ij} and k_{ij}. The presence or absence of a rising phase is determined entirely by whether the I_g amplitude for the second transition is greater or less than that for the first. The issue is that $I_g(t)$ for the second transition develops with a delay while the total gating current is just the sum for each transition. The amplitude of I_g for the closed$_1$-open transition can be increased and hence a rising phase generated either by increasing the charge displaced for each transition (Q_{10}) or the number of transitions per unit time (k_{10}).

$I_{Na}(t)$ can be sensitive or insensitive to the order of the forward rate constants

Armstrong (1981) and Armstrong and Matteson (1984) also found that $I_{Na}(t)$ was insensitive to the order of the rate constants when the steady-state probability of occupancy of the conducting state was near unity. It is shown in the Appendix that this insensitivity is an inherent property of the kinetic scheme when the steady-state occupancy is 1.0 (i.e. $k_{01} = 0$), and does not depend on the values selected for the other rate constants under these initial conditions. This insensitivity to the order is not a general property of the scheme, however. When the steady-state occupancy of the conducting state is <1.0, $I_{Na}(t)$ can be more or less sensitive to order depending on the values selected for the rate constants. This is discussed briefly in the Appendix and illustrated in Figs. 10 *D* and *E*.

Fig. 10 *D* presents computations of $I_{Na}(t)$ and $I_g(t)$ with $k_{21} = 10.0$ ms^{-1}, $k_{12} = 0.05$ ms^{-1}, $k_{10} = 1.67$ ms^{-1}, and $k_{01} = 1.6617$ ms^{-1} (indicated by $k_{21} > k_{10}$), and again with the values of k_{21} and k_{10} exchanged each for each. For the second computation k_{01} was increased to 9.7093 ms^{-1} to keep the steady-state occupancy of the conducting state at 0.5 throughout. There is a clear effect on $I_{Na}(t)$. A

rising phase is not generated in I_g because Q_{21}/Q_{10} was set to 4.0.

Fig. 10 *E* presents two computations of $I_{Na}(t)$ and $I_g(t)$ using the parameters for the second two transitions of Armstrong and Matteson (1984). Their k_{01} value has been set to zero to keep the steady-state occupancy of the conducting state at unity. Computations are presented with k_{21} and k_{10} in the ratio 2:1 (14.2 and 7.16 ms^{-1}) and again in the ratio 2:3 (14.3 and 21.5 ms^{-1}). $I_g(t)$ was computed assuming only the closed$_2$-closed$_1$ transition was voltage dependent. There are clear effects on $I_{Na}(t)$ while the two $I_g(t)$ computations are indistinguishable, the opposite result to that obtained by Armstrong and Matteson. The divergent results are an artefact of the parameters selected. The effects on $I_{Na}(t)$ seen here were compensated for in Armstrong and Matteson's simulations by adding a rapid delaying relaxation in the 2:1 case and a much slower one in the 2:3 case. $I_g(t)$ for the 2:1 case is given by

$$I_g(t) = 14.2NQ_{21}[0.9933 \exp(-t/0.070) + 0.0067 \exp(-t/0.141)], \quad (5)$$

and for the 2:3 case by

$$I_g(t) = 14.3NQ_{21}[0.1258 \exp(-t/0.044) + 0.8742 \exp(-t/0.074)]. \quad (6)$$

The dominant relaxations in Eqs. 5 and 6 have very similar time constants. This illustrates the difficulty in coming to general conclusions with simulations using any particular set of parameters. With only the results of Fig. 10 *E* at hand one might have concluded that I_{Na} is but I_g is not sensitive to the order of the forward rate constants.

I_{Na} tail currents provide kinetic information

It is shown in the Appendix that two closed and a single open state are sufficient to require that, in general, I_{Na} tail current will decay as the sum of two exponentials. Multiple tail current components have sometimes been taken as direct evidence for multiple open states, (e.g. Armstrong and Bezanilla, 1977; see also Armstrong, 1981; Armstrong and Matteson, 1984). However, such observations are not of themselves sufficient to require more than one open state. For the case that the steady-state occupancy of the conducting state reaches zero at OFF, I_{Na} can decay as either one or two exponentials depending on which of the forward transition rate constants is zero (see Appendix).

In *Myxicola* there is more than one tail current component both at potentials where the Na conductance is and is not zero (Goldman and Hahin, 1978). There are at least two closed states as there is a delay in the rise of I_{Na} and for this reason alone multiple tail current components are expected. For I_g, two closed and a single conducting state are sufficient to require two OFF relaxations whatever the steady-state occupancy of the conducting state (see Appendix, Eq. A22). The OFF time constants for both I_{Na} and I_g agree fairly closely. The simplest way to account for the available data, then, is to treat the two recognized OFF components as arising from two closed states. Oxford (1981) could describe tail currents in squid with a single exponential. However, he found that systematic changes in initial conditions produced systematic changes in the value of the fitted exponential, suggesting unresolved components. A difference between squid and *Myxicola,* then, is that the OFF components for both I_{Na} and I_g seem to be better separated in *Myxicola.*

OFF currents were computed using Eqs. A17 and A22 with $k_{12} = 3.8\ ms^{-1}$, $k_{10} = 1.5\ ms^{-1}$, $k_{01} = 12.5\ ms^{-1}$, and $k_{21} = 0$ yielding time constants of 60 and 306 μs (Fig. 10 *F*, indicated by $k_{12} < k_{01}$, lower traces are I_{Na} and upper are I_g). For I_{Na} the ratio of the amplitudes of the slow to the fast relaxation was 0.22 in good agreement with the experimental value of 0.26 (Table 3). For I_{OFF} with $Q_{21} = Q_{10}$ the ratio was 0.63 in rough agreement with the experimental mean of 0.42 (Table 1). Note (Eq. A22) that if only the closed$_2$-closed$_1$ transition is voltage dependent then the predicted ratio of relaxation amplitudes in I_{OFF} is always unity whatever the values of the rate constants. Definite conclusions cannot be drawn however, because the value of Q_{21}/Q_{10} is not known.

A more useful result is obtained from the ratio of relaxation amplitudes in the Na tail current as this depends only on the rate constants, given these initial conditions. Inverting the values for k_{01} and k_{12} has no effect on *a* or *b* (Eqs. A7 and A8), but will in general change the coefficients. Computations with $k_{12} = 12.5\ ms^{-1}$ and $k_{01} = 3.8\ ms^{-1}$ (indicated by $k_{12} > k_{01}$) yielded a ratio of slow to fast relaxation amplitudes of 20.2, sharply divergent from the experimental results. The I_{OFF} response now had a rising phase. The condition for the slow relaxation amplitude to be small relative to the fast is that k_{01} is close to *a* and far from *b.* Extensive computations indicated that this condition is produced with $k_{01} > k_{12}$. A small slow/fast amplitude ratio was never produced with $k_{12} > k_{01}$, and the ratio decreased with increasing k_{01}/k_{12} values. The experimental tail current results are, then, consistent with $k_{01} > k_{12}$ at −100 mV.

CONCLUSIONS

Under the assumptions stated each relaxation in I_g should also appear in I_{Na}. The origin of the slow ON component in gating currents from squid, canine Purkinje cells, and *Myxicola* is then a significant question to be resolved. A step toward resolution may be provided by the finding that there seems to be more than two or three components in the ON of the gating current. In both squid and canine cardiac Purkinje cells (Bezanilla et al., 1982; Stimers et al., 1987; Hanck et al., 1990) more positive holding or conditioning potentials speeded $\tau_{ON\text{-}F}$.

APPENDIX

Na current

For the scheme presented in Discussion, let x_2 be the probability of occupancy of state closed$_2$, x_1 the probability of occupancy of state closed$_1$ and x_0 the probability of occupancy of the open state. Then,

$$\dot{x}_2 = -k_{21}x_2 + k_{12}x_1 \tag{A1}$$

$$\dot{x}_1 = -(k_{12} + k_{10})x_1 + k_{21}x_2 + k_{01}x_0 \tag{A2}$$

$$\dot{x}_0 = -k_{01}x_0 + k_{10}x_1. \tag{A3}$$

Using the required condition that

$$x_2 + x_1 + x_0 = 1, \tag{A4}$$

any one of the variables can be eliminated, and the remaining two coupled first order equations combined into the single second order equation

$$\ddot{x}_i + (a + b)\dot{x}_i + ab[x_i - x_i(\infty)] = 0. \tag{A5}$$

x_i is the probability of occupancy of any selected state, $x_i(\infty)$ is its steady-state probability of occupancy and a and b are given by Eqs. A7 and A8.

A solution to Eq. A5 is given by

$$x_i(t) = x_i(\infty) - \left\{\frac{\dot{x}_i(0) + b[x_i(0) - x_i(\infty)]}{a - b}e^{-at}\right\} + \left\{\frac{\dot{x}_i(0) + a[x_i(0) - x_i(\infty)]}{a - b}e^{-bt}\right\} \tag{A6}$$

with

$$a = \frac{k_{21} + k_{12} + k_{10} + k_{01}}{2} + \left[\left(\frac{k_{21} + k_{12} + k_{10} - k_{01}}{2}\right)^2 + (k_{01} - k_{21})k_{10}\right]^{1/2} \tag{A7}$$

$$b = \frac{k_{21} + k_{12} + k_{10} + k_{01}}{2} - \left[\left(\frac{k_{21} + k_{12} + k_{10} - k_{01}}{2}\right)^2 + (k_{01} - k_{21})k_{10}\right]^{1/2} \tag{A8}$$

$x_i(0)$ is the probability of occupancy of the selected state at $t = 0$, and the time derivative of the initial probability of occupancy, $\dot{x}_i(0)$, is given by either Eq. A1, A2, or A3 evaluated at $t = 0$. We have

$$x_2(\infty) = k_{12}k_{01}/(k_{21}k_{10} + k_{21}k_{01} + k_{12}k_{01}) \tag{A9}$$

$$x_1(\infty) = k_{21}k_{01}/(k_{21}k_{10} + k_{21}k_{01} + k_{12}k_{01}) \tag{A10}$$

$$x_0(\infty) = k_{21}k_{10}/(k_{21}k_{10} + k_{21}k_{01} + k_{12}k_{01}). \tag{A11}$$

$I_{Na}(t)$ is then given by

$$I_{Na}(t) = Ni_{Na}x_0(t), \tag{A12}$$

where i_{Na} is the current through a single open channel, and N is the channel density.

There are a few special cases of interest. For the ON of I_{Na} assuming that $x_2(0) = 1.0$, then $x_1(0) = x_0(0) = 0, \dot{x}_0(0) = 0$ and Eq. A12 becomes

$$I_{Na}(t) = Ni_{Na}\left[x_0(\infty) + \frac{bx_0(\infty)}{a - b}e^{-at} - \frac{ax_0(\infty)}{a - b}e^{-bt}\right]. \tag{A13}$$

With $k_{01} = 0$, then $x_0(\infty) = 1.0$, the conducting state is absorbing, and

$$I_{Na}(t) = Ni_{Na}\left[1 + \frac{b}{a - b}e^{-at} - \frac{a}{a - b}e^{-bt}\right]. \tag{A14}$$

Under these conditions, exchanging the numerical values of the forward rate constants, k_{21} and k_{10}, with each other (i.e., inverting the order of the rate constants) has no effect on the values of the relaxation rate constants, a and b, as these terms now only appear as a product or sum in Eqs. A7 and A8. Hence $I_{Na}(t)$ would be unchanged as it is determined entirely by a and b. In general, when k_{01} is not negligible, $I_{Na}(t)$ can be sensitive to the order of the forward rate constants owing to the k_{10} $(k_{01} - k_{21})$ terms in Eqs. A7 and A8. In this more general case the degree of sensitivity is dependent on the particular values of the rate constants selected. For example, with $k_{10} = k_{10}$ and $k_{12} = 0$, then $x_0(\infty)$ is 0.5. In this case $I_{Na}(t)$ is more or less sensitive to order depending on whether the ratio k_{21}/k_{10} is near or far from unity.

For Na tail currents assuming $x_0(0) = 1.0$, then $\dot{x}_0(0) = -k_{01}$, and $I_{Na}(t)$ is given by

$$I_{Na}(t) = Ni_{Na} \cdot \left\{x_0(\infty) - \frac{b[1 - x_0(\infty)] - k_{01}}{a - b}e^{-at} + \frac{a[1 - x_0(\infty)] - k_{01}}{a - b}e^{-bt}\right\}. \tag{A15}$$

Hence two closed and only one conducting state require two deactivation relaxations when $x_0(\infty)$ is not zero. When $x_0(\infty)$ is zero there are one or two deactivation relaxations depending on whether k_{10} or k_{21} has become zero. In the first case a becomes $(k_{21} + k_{12})$ and b becomes k_{01}. Eq. A15 then becomes

$$I_{Na}(t) = Ni_{Na}\exp(-k_{01}t), \tag{A16}$$

a single exponential determined only by the k_{01} back rate constant. With $k_{21} = 0$, Eq. A15 becomes

$$I_{Na}(t) = Ni_{Na} \cdot \left[-\frac{b - k_{01}}{a - b} \exp(-at) + \frac{a - k_{01}}{a - b} \exp(-bt) \right]. \quad \text{(A17)}$$

Under these initial conditions Eq. A17 is always the sum of exponentials.

Gating current

For the closed$_2$-closed$_1$ transition the charge displaced is proportional to $(x_1[t] - x_1[0])$ less the change in occupancy of closed$_1$ owing to interactions with the open state. We have

$$Q'_g(t) = NQ_{21} \left\{ x_1(t) - x_1(0) - \int_0^t [k_{01}x_0(t) - k_{10}x_1(t)]\, dt \right\}, \quad \text{(A18)}$$

where Q_{21} is the charge displaced when a single channel makes the transition from closed$_2$ to closed$_1$. $I_g(t)$ is given by the derivative of Eq. A18, substituting from Eq. A2,

$$I'_g(t) = NQ_{21}\,[k_{21}x_2(t) - k_{12}x_1(t)]. \quad \text{(A19)}$$

Proceeding in a similar way for the closed$_1$-open transition

$$I''_g(t) = NQ_{10}[k_{10}x_1(t) - k_{01}x_0(t)], \quad \text{(A20)}$$

where the $x_0(t)$, etc. terms are given by Eq. A6. Total gating current, $I_g(t)$ is then the sum of Eqs. A19 and A20.

A special case of interest is the ON response assuming $x_2(0) = 1.0$. $I_g(t)$ is then given by

$$I_g(t) = k_{21}N \left[\frac{Q_{21}(k_{21} + k_{12} - b) - Q_{10}k_{10}}{a - b} e^{-at} - \frac{Q_{21}(k_{21} + k_{12} - a) - Q_{10}k_{10}}{a - b} e^{-bt} \right]. \quad \text{(A21)}$$

Note that Eq. A21 is identical in form with either $x_0(\infty) = 1.0$ or $x_0(\infty)$ any smaller value. However, the interpretations of a and b will change. For the OFF response, assuming $x_0(0) = 1.0$, $I_g(t)$ is

$$I_g(t) = k_{01}N \left[\frac{Q_{10}(b - k_{01} - k_{10}) + Q_{21}k_{12}}{a - b} e^{-at} - \frac{Q_{10}(a - k_{10} - k_{01}) + Q_{21}k_{12}}{a - b} e^{-bt} \right]. \quad \text{(A22)}$$

Note that for two closed and a single open state, I_g at OFF always decays as two exponentials even when $x_0(\infty) = 0$ and irrespective of whether k_{10} or k_{21} is zero.

I thank Ben Deardorff for assistance with some of the experiments and for his continued interest in the project, Jeff Michaels for design and construction of some of the electronic equipment, and Drs. R. W. Hadley, W. J. Lederer, and M. F. Schneider for comments on the manuscript.

This work was supported by National Institutes of Health grant NS 07734.

Received for publication 8 June 1990 and in final form 17 September 1990.

REFERENCES

Alicata, D. A., M. D. Rayner, and J. G. Starkus. 1989. Osmotic and pharmacological effects of formamide on capacity current, gating current and sodium current in crayfish giant axons. *Biophys. J.* 55:347–353.

Alicata, D. A., M. D. Rayner, and J. G. Starkus. 1990. Sodium channel activation mechanisms. Insights from deuterium oxide substitution. *Biophys. J.* 57:745–758.

Armstrong, C. M. 1981. Sodium channels and gating currents. *Physiol. Rev.* 61:644–683.

Armstrong, C. M., and F. Bezanilla. 1973. Currents related to movement of the gating particles of the sodium channels. *Nature (Lond.).* 242:459–461.

Armstrong, C. M., and F. Bezanilla. 1974. Charge movement associated with the opening and closing of the activation gates of the Na channels. *J. Gen. Physiol.* 63:533–552.

Armstrong, C. M., and F. Bezanilla. 1975. Currents associated with the ionic gating structures in nerve membrane. *Annu. NY Acad. Sci.* 264:265–277.

Armstrong, C. M., and F. Bezanilla. 1977. Inactivation of the sodium channel. II. Gating current experiments. *J. Gen. Physiol.* 70:567–590.

Armstrong, C. M., and W. F. Gilly. 1979. Fast and slow steps in the activation of sodium channels. *J. Gen. Physiol.* 74:691–712.

Armstrong, C. M., and D. R. Matteson. 1984. Sequential models of sodium channel gating. *In* Current Topics in Membranes and Transport. P. F. Baker, editor. Academic Press, Orlando, FL. 22:331–352.

Bekkers, J. M., I. C. Forster, and N. G. Greeff. 1989. High resolution recording of Na gating currents from squid reveal a fast initial component. *Biophys. J.* 55:316*a*. (Abstr.)

Bezanilla, F., and C. M. Armstrong. 1974. Gating currents of the sodium channel: three ways to block them. *Science (Wash. DC).* 183:753–754.

Bezanilla, F., and C. M. Armstrong. 1975. Kinetic properties and inactivation of the gating currents of sodium channels in squid axon. *Phil. Trans. Roy. Soc. Lond. B.* 270:449–458.

Bezanilla, F., R. E. Taylor, and J. M. Fernández. 1982. Distribution and kinetics of membrane dielectric polarization. I. Long-term inactivation of gating currents. *J. Gen. Physiol.* 79:21–40.

Binstock, L., and L. Goldman. 1969. Current and voltage-clamped studies on *Myxicola* giant axons. Effect of Tetrodotoxin. *J. Gen. Physiol.* 54:730–740.

Bullock, J. O., and C. L. Schauf. 1978. Combined voltage-clamp and dialysis of *Myxicola* axons; behavior of membrane asymmetry currents. *J. Physiol. (Lond.).* 278:309–324.

Bullock, J. O., and C. L. Schauf. 1979. Immobilization of intramembrane charge in *Myxicola* giant axons. *J. Physiol. (Lond.).* 286:157–172.

Campbell, D. T. 1983. Sodium channel gating currents in frog skeletal muscle. *J. Gen. Physiol.* 82:679–702.

Chiu, S. Y. 1980. Asymmetry currents in the mammalian myelinated nerve fiber. *J. Physiol. (Lond.).* 309:499–520.

Colquhoun, D. 1971. Lectures in Biostatistics. An Introduction to Statistics with Applications in Biology and Medicine. Clarendon Press, Oxford. 425 pp.

Dubois, J. M., and M. F. Schneider. 1982. Kinetics of intramembrane charge movement and sodium current in frog node of Ranvier. *J. Gen. Physiol.* 79:571–602.

Ebert, G. A., and L. Goldman. 1975. Internal perfusion of the *Myxicola* giant axon. *Biophys. J.* 15:495–499.

Forster, I. C., and N. G. Greeff. 1990. Properties of a fast displacement charge recorded from the squid giant axon. *Biophys. J.* 57:105*a*. (Abstr.)

Gillespie, J. I., and H. Meves. 1980. The time course of sodium inactivation in squid giant axons. *J. Physiol.* (*Lond.*). 299:289–308.

Gilly, W. F., and C. M. Armstrong. 1982. Slowing of sodium channel opening kinetics of squid axon by extracellular zinc. *J. Gen. Physiol.* 79:935–964.

Gilly, W. F., and C. M. Armstrong. 1984. Threshold channels—a novel type of sodium channel in squid giant axon. *Nature* (*Lond.*). 309:448–450.

Goldman, L. 1986. Internal cesium and the sodium inactivation gate in *Myxicola* giant axons. *Biophys. J.* 50:231–238.

Goldman, L. 1989. Sodium channel opening as a precursor to inactivation. A route to the inactivated state. *Eur. Biophys. J.* 16:321–325.

Goldman, L. 1990. Gating current kinetics in *Myxicola* giant axons. *Abstr. 10th Int. Biophys. Cong., Vancouver.* In press.

Goldman, L., and R. Hahin. 1978. Initial conditions and the kinetics of the sodium conductance in *Myxicola* giant axons. II. Relaxation experiments. *J. Gen. Physiol.* 72:879–898.

Goldman, L., and J. L. Kenyon. 1979. Internally perfused *Myxicola* giant axons showing long-term survival. *Biophys. J.* 28:357–362.

Goldman, L., and C. L. Schauf. 1973. Quantitative description of sodium and potassium currents and computed action potentials in *Myxicola* giant axons. *J. Gen. Physiol.* 61:361–384.

Hahin, R. 1988. Removal of inactivation causes time-invariant sodium current decays. *J. Gen. Physiol.* 92:331–350.

Hahin, R., and L. Goldman. 1978. Initial conditions and the kinetics of the sodium conductance in *Myxicola* giant axons. I. Effects on the time-course of the sodium conductance. *J. Gen. Physiol.* 72:863–877.

Hanck, D. A., M. F. Sheets, and H. A. Fozzard. 1990. Gating currents associated with Na channels in canine cardiac Purkinje cells. *J. Gen. Physiol.* 95:439–457.

Keynes, R. D. 1986. Modelling the sodium channel. *In* Ion Channels in Neural Membranes. Alan R. Liss, New York. 85–101.

Keynes, R. D., and J. E. Kimura. 1983. Kinetics of activation of the sodium conductance in the squid giant axon. *J. Physiol.* (*Lond.*). 336:621–634.

Keynes, R. D., and E. Rojas. 1974. Kinetics and steady-state properties of the charged system controlling sodium conductance in the squid giant axon. *J. Physiol.* (*Lond.*). 239:393–434.

Kimura, J. E., and H. Meves. 1979. The effect of temperature on the asymmetrical charge movement in squid giant axons. *J. Physiol.* (*Lond.*). 289:479–500.

Meves, H. 1974. The effect of holding potential on the asymmetry currents in squid giant axons. *J. Physiol.* (*Lond.*). 243:847–867.

Mozhaeva, G. N., A. P. Naumov, and E. D. Nosyreva. 1980. Kinetics of sodium tail current during repolarization of axon membrane normally and in the presence of scorpion toxin. *Neirofiziolgiia.* 12:541–549.

Neumcke, B., W. Nonner, and R. Stämpfli. 1976. Asymmetrical displacement current and its relation with the activation of sodium current in the membrane of frog myelinated nerve. *Pfluegers Arch. Eur. J. Physiol.* 363:193–203.

Nonner, W. 1980. Relations between the inactivation of sodium channels and the immobilization of gating charge in frog myelinated nerve. *J. Physiol.* (*Lond.*). 299:573–604.

Nonner, W., E. Rojas, and R. Stämpfli. 1978. Asymmetrical displacement currents in the membrane of frog myelinated nerve: early time course and effects of membrane potential. *Pfluegers Arch. Eur. J. Physiol.* 375:75–85.

Oxford, G. S., 1981. Some kinetic and steady-state properties of sodium channels after removal of inactivation. *J. Gen. Physiol.* 77:1–22.

Pohl, J. A. 1989. Recovery from charge immobilization in sodium channels of the frog node of Ranvier. *Pfluegers Arch. Eur. J. Physiol.* 414:516–522.

Rudy, B. 1976. Sodium gating currents in *Myxicola* giant axons. *Proc. Roy. Soc. Lond. B.* 193:469–475.

Rudy, B. 1981. Inactivation in *Myxicola* giant axons responsible for slow and accumulative adaptation phenomena. *J. Physiol.* (*Lond.*). 312:531–550.

Schauf, C. L. 1983. Evidence for negative gating charges in *Myxicola* axons. *Biophys. J.* 42:225–232.

Schauf, C. L. 1987. Selective modification of sodium channel gating by solvents and drugs. *Eur. J. Pharmacol.* 136:89–95.

Schauf, C. L., and J. O. Bullock. 1979. Modifications of sodium channel gating in *Myxicola* giant axons by deuterium oxide, temperature, and internal cations. *Biophys. J.* 27:193–208.

Sigworth, F. J. 1981. Covariance of nonstationary sodium current fluctuations at the node of Ranvier. *Biophys. J.* 34:111–134.

Starkus, J. G., B. D. Fellmeth, and M. D. Rayner. 1981. Gating currents in the intact crayfish giant axon. *Biophys. J.* 35:521–533.

Stimers, J. R., F. Bezanilla, and R. E. Taylor. 1987. Sodium channel gating currents. Origin of the rising phase. *J. Gen. Physiol.* 89:521–540.

Swenson, R. P. 1983. A slow component of gating current in crayfish giant axons resembles inactivation charge movement. *Biophys. J.* 41:245–250.

Taylor, R. E., and F. Bezanilla. 1983. Sodium and gating current time shifts resulting from changes in initial conditions. *J. Gen. Physiol.* 81:773–784.